Emulsion polymerization in various reactor types: recipes with high monomer contents

Pergamon

Chemical Engineering Science, Vol. 49, No. 24B, pp. 4971–4980, 1994

0009–2509/94 $7.00 + 0.00

0009–2509(94)00272–X

EMULSION POLYMERIZATION IN VARIOUS REACTOR TYPES: RECIPES WITH HIGH MONOMER CONTENTS

M. J. J. MAYER, J. MEULDIJK* and D. THOENES
Laboratory of Chemical Process Technology, Eindhoven University of Technology, PO Box 513, 5600 MB Eindhoven, The Netherlands

(*Received* 11 *June 1994*; *accepted for publication* 12 *September* 1994)

Abstract—The effect of the monomer content in the recipe on the emulsion polymerization of styrene has been studied in a batch reactor, a continuously operated stirred tank reactor (CSTR) and a pulsed packed column (PPC). In a pulsed packed column, which has been developed in the authors' laboratory, a good local agitation is combined with little backmixing.

The results of this study show that the maximum volume of the particle phase at which isothermal reactor operation is possible, depends significantly on the particle size distribution. In fact, a limited degree of backmixing appears to have a favourable effect. Therefore, the PPC is a promising reactor for continuous emulsion polymerization, provided there is sufficient radial mixing.

INTRODUCTION

Commercial emulsion polymerization reactions are usually carried out in batch or semi-batch reactors. In such reactors, an almost complete conversion can be obtained and preparation of different products is possible in the same reactor. For the production of large amounts of the same product, the use of a continuously operated stirred tank reactor (CSTR) may be preferable. However, as a result of residence time distribution, the emulsion polymerization in a CSTR leads to products with a much lower monomer conversion, a lower particle concentration and a much broader particle size distribution as compared to batch reactors (DeGraff and Poehlein, 1971; Nomura *et al.*, 1971).

In a pulsed packed column (PPC), which has been developed in the authors' laboratory, a good local agitation is combined with little backmixing. In the PPC, the conversions and the particle concentrations of the batch process can be approached for styrene and vinyl acetate emulsion polymerization (Hoedemakers and Thoenes, 1990; Meuldijk *et al.*, 1992).

The work summarized in this paper describes the influence of the monomer weight fraction in the recipe on the performance of a batch reactor, a CSTR and a PPC.

POLYMERIZATION RATE

The overall polymerization rate R_p of a latex with a discrete particle size distribution divided into k particle size classes is given by:

$$R_p = \frac{k_p C_{Mp} \sum_{i=1}^{k} N_i \bar{n}_i}{N_{Av}} \tag{1}$$

where k_p is the propagation rate constant, C_{Mp} is the monomer concentration in the particles, N_i is the number of particles in particle size class i per unit volume of the continuous phase, $\bar{n}_i$ is the time averaged number of growing chains per particle in particle size class i and N_{Av} is Avogadro's number.

PARTICLE NUMBER

Batch process

For the stage of the polymerization process where no new particles are formed and the existing particles grow at the expense of the monomer droplets (interval 2), Smith and Ewart (1948) derived the following relation for the polymerization rate and the particle number:

$$N \propto R_p \propto C_{I0}^{0.4}(C_{E0} - C_{CMC})^{0.6} C_{M0}^{0} \tag{2}$$

where C_{I0}, C_{E0} and C_{M0}, respectively, stand for the "concentrations", i.e. amounts per unit volume of water of the initiator, the emulsifier and the monomer. C_{CMC} is the critical micelle concentration.

Relation 2 is based on the assumptions of the so-called "Case 2" kinetics:

- The time averaged number of growing chains per particle equals 0.5 and is independent of the particle size.
- Particle nucleation stops when all emulsifier is adsorbed onto the particle surface.

*To whom correspondence should be addressed

Process in the CSTR

As a result of the residence time distribution in a CSTR, freshly added emulsifier is mixed up with rather large particles that adsorb emulsifier for colloidal stabilization. Therefore, only part of the emulsifier is available for the generation of new particles, leading to a lower particle number as compared to a batch process with the same recipe.

DeGraff and Poehlein (1971) derived a relation for the number of particles and the polymerization rate in the steady state for the emulsion polymerization in a CSTR, accounting for the particle size distribution resulting from the residence time distribution:

$$N \propto R_p \propto (C_{E0} - C_{CMC})C_{I0}^{0}C_{M0}^{0}\tau^{-2/3} \qquad (3)$$

where τ is the mean residence time in the CSTR. Relation 3 is based on Smith–Ewart "Case 2" kinetics and the assumption that the rate of radical absorption into micelles and existing particles is proportional to their surface area.

Process in the PPC

The emulsion polymerization of styrene in a pulsed packed column can be described in terms of a differential balance for the nucleated particles and differential mass balances for the monomer and the emulsifier. These balances are based on the plug flow with the axial dispersion model for the residence time distribution (Mayer, 1995). The number of particles nucleated in the PPC depends considerably on the residence time distribution, e.g. the pulsation conditions, and has a value between the particle number of the batch process and the process in the CSTR. For this study it is sufficient to note that the polymerization rate at axial position $z[R_p(z)]$ can be calculated through a mass balance for the monomer over an element of the column with a length dz:

$$R_p(z) = \frac{k_p C_{Mp}(z)\sum_{i=1}^{k} N_i(z)\bar{n}_i(z)}{N_{Av}} = uC_{M0}\frac{dX(z)}{dz} - EC_{M0}\frac{d^2X(z)}{dz^2} \qquad (4)$$

where u, X and E stand for the interstitial fluid velocity, the conversion and the axial dispersion coefficient, respectively. The axial dispersion coefficient (E) is related to the stroke length (s) and the frequency of pulsation (f) (Hoedemakers, 1990).

DEVIATIONS FROM SMITH–EWART CASE 2 KINETICS

The assumption that the average number of growing chains per particle $\bar{n}$ equals 0.5 is only valid if:

- the radical desorption rate is negligible with respect to the radical absorption rate, and
- instantaneous bimolecular termination occurs when a second radical enters a growing particle.

During particle nucleation, when the particles are still small, the value of $\bar{n}$ is less than 0.5, because a significant number of radicals desorb from the growing particles before the absorption of a second radical leads to instantaneous termination.

On the other hand, for large particles at relatively high conversions, the assumption that instantaneous bimolecular termination takes place when a second radical enters a growing particle is not valid. In this situation, the value of $\bar{n}$ is greater than 0.5. When Smith–Ewart Case 2 kinetics are not valid, the average number of growing chains per particle $\bar{n}$ can be calculated through a radical population balance over the particle size distribution, leading to the Smith and Ewart (1948) recursion relation:

$$\frac{\rho_{a,i}N_{Av}}{N_i}(N_{i,n-1} - N_{i,n}) + k_{des,i}[(n+1)N_{i,n+1} - nN_{i,n}] + \frac{k_t}{v_{p,i}N_{Av}}[(n+2)(n+1)N_{i,n+2} - n(n-1)N_{i,n}] = 0 \qquad (5)$$

in which $N_{i,n}$, $v_{p,i}$, $\rho_{a,i}$ and $k_{des,i}$ stand for the number of particles, the particle volume, the radical entry rate, and the rate coefficient for radical desorption from the particles, respectively, all for particle size class, i. The rate constant for bimolecular termination is k_t.

Stockmayer (1957) and O'Toole (1967) derived the following equation for the time averaged number of growing chains per particle ($\bar{n}_i$) in size class i:

$$\bar{n}_i = \frac{a}{4}\frac{I_b(a)}{I_{b-1}(a)} \qquad (6)$$

where $I_b(a)$ is a modified Bessel function of the first kind, of order b and argument a. The values of a and b are given by:

$$a = 2\left(\frac{2v_{p,i}N_{Av}^2\rho_{a,i}}{N_i k_t}\right)^{0.5} \qquad (7)$$

and

$$b = \frac{v_{p,i}N_{Av}k_{des,i}}{k_t}. \qquad (8)$$

According to Ugelstad *et al.* (1967) the overall rate of radical absorption (ρ_a) can be expressed in terms of radical formation in the water phase (ρ_i), radical desorption from the particles and termination of radicals in the water phase. For a latex with k particle size classes the radical absorption rate may be represented by:

$$\rho_a = \rho_i + \frac{\sum_{i=1}^{k} k_{des,i}N_i\bar{n}_i}{N_{Av}} - 2k_{tw}C_{rw}^2 \qquad (9)$$

where C_{rw} is the radical concentration in the water phase.

For the recipes investigated, termination of radicals in the water phase is negligible with respect to radical desorption and radical production in the water phase. As a consequence, the third term on the right-hand side of eq. (9) may be neglected.

Friis and Nyhagen (1973), Nomura and Harada (1981) and Asua *et al.* (1991) derived expressions for the rate of radical desorption from the particles into

the water phase. For situations where the mass transfer rate of the (small) radicals from the particles into the water phase is much less than the propagation rate of the radicals, i.e. for sparingly water-soluble monomers such as styrene, the following equation has been found for the desorption rate of particles in size class i:

$$k_{des,i} = \frac{3D_m \frac{k_{tr}}{k_p}}{\left(\frac{d_{p,i}}{2}\right)^2} \quad (10)$$

in which D_m is the effective diffusivity of the (small) radicals and k_{tr} is the effective chain transfer rate constant.

If each of the parameters k_p, ρ_i, k_t, D_m, k_{tr} and the particle size distribution are known, the polymerization rate of a latex with any particle size distribution can be calculated through eq. (1) and eqs. (6)–(10).

EXPERIMENTAL

The chemicals used in this study were distilled water, distilled commercial-grade styrene, commercial-grade sodium dodecyl sulphate and laboratory-grade sodium persulphate. The reaction temperature was 50°C, the pH of the reaction mixture was 5.5 and the applied impeller speed was 500 rpm. The batch reactor and the CSTR were both stainless steel tanks equipped with an eight-bladed Rushton impeller and four baffles. Unless stated otherwise, the volumes of the batch reactor and the CSTR were 1.2 and 2.4 dm^3, respectively. During the polymerization, samples were taken for the determination of the conversion by gravimetry and the particle size distribution by transmission electron microscopy.

Figure 1 shows a schematic view of the pilot installation with the PPC. The column (length, 5.1 m; internal diameter, 0.05 m) was packed with Raschig rings (diameter, 0.01 m; bed porosity, 0.73), equipped with a thermostatted water jacket and six sample points. The pulsation frequency was 3.5 s^{-1} and the stroke length in the column was varied between 6.9×10^{-3} m and 13.8×10^{-3} m. For the rheological measurements, a Contraves Rheomat 115 rotation viscosimeter was used.

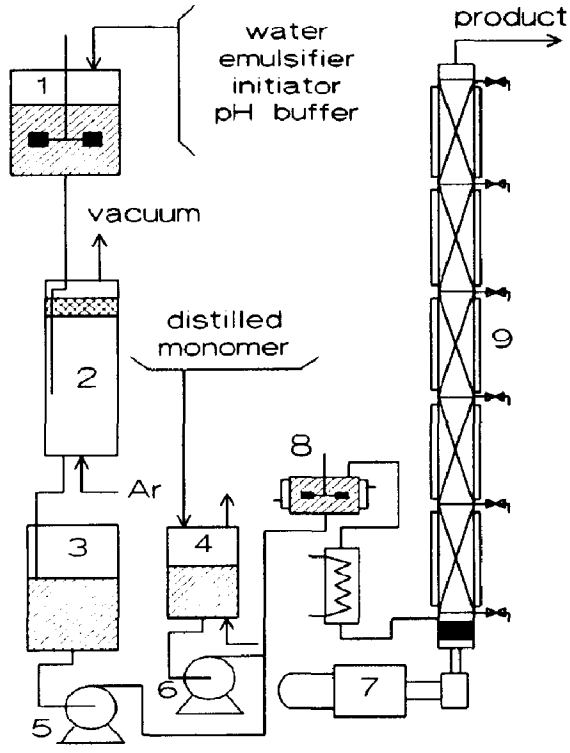

Fig. 1. The pulsed packed column equipment. 1, Mixing vessel for the preparation of the continuous phase; 2, bubble column; 3 and 4, storage vessels; 5 and 6, pumps; 7, pulsator; 8, premixer; 9, packed column.

RESULTS

Batch process

Figures 2(a) and 2(b), respectively, show the course of the particle number and the polymerization rate in interval 2 as a function of $(C_{E0} - C_{CMC})^{0.6} C_{I0}^{0.4}$ [eq. (2)] for the batch experiments summarized in Table 1. Figures 2(a) and 2(b) show that both the particle number and the polymerization rate in interval 2 are well predicted by the classical Smith–Ewart theory [see eq. (2)] for styrene weight fractions in the recipe below 0.45. However, for styrene weight fractions in the recipe above 0.45, the polymerization rate appeared to be higher for higher monomer contents despite the zeroth-order kinetics in this stage of the process. In Fig. 2(b) it can also be seen that this effect of the monomer weight fraction in the recipe on the polymerization rate strongly increases with the dimensions of the reactor. Note that the particle number is predicted by the Smith–Ewart relation for all recipes studied.

Figure 3 shows the rheological behaviour of the latex product obtained from a batch experiment with a monomer weight fraction of 0.47 in the recipe (see Table 1). The particle size distribution of the latex used for the rheological measurements in Fig. 3 is given in Fig. 4. Rheological measurements for recipes with monomer weight fractions lower than 0.47, but with the same initiator and emulsifier concentration, were performed by dilution of the latex product with distilled water.

Figure 3 reveals a pseudoplastic rheological behaviour for latexes with a particle volume fraction above 0.4. This pseudoplastic behaviour originates from the orientation of the latex particles in the direction of shear. In accordance with Mooney (1951) and Sadler and Sim (1991), the latexes with particle volume fractions above 0.4 show a very strong increase of the apparent viscosity with the volume fraction of the particle phase, which may result in a change from turbulent to laminar flow in the later

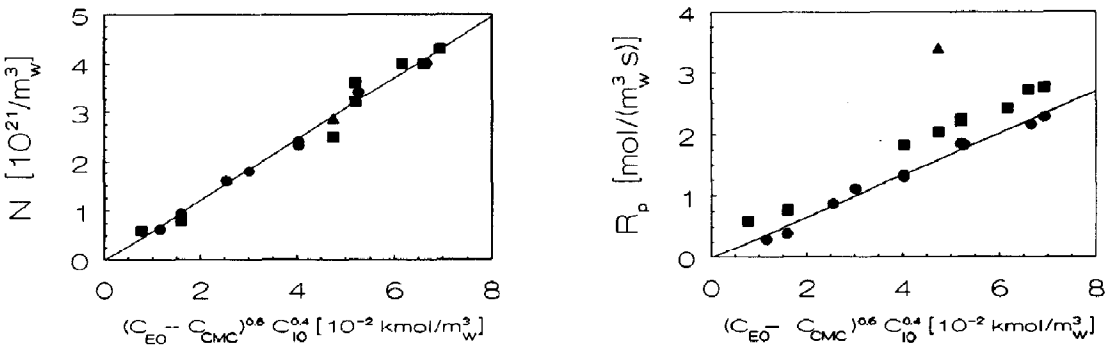

Fig. 2. (a) The particle number N and (b) the polymerization rate R_p as a function of the term $(C_{E0} - C_{CMC})^{0.6} C_{I0}^{0.4}$ for the batch experiments listed in Table 1. ●, $f_m < 0.45$, $V_{reactor} = 1.2\,dm^3$; ■, $f_m \geq 0.45$, $V_{reactor} = 1.2\,dm^3$; ▲, $f_m = 0.47$, $V_{reactor} = 2.4\,dm^3$.

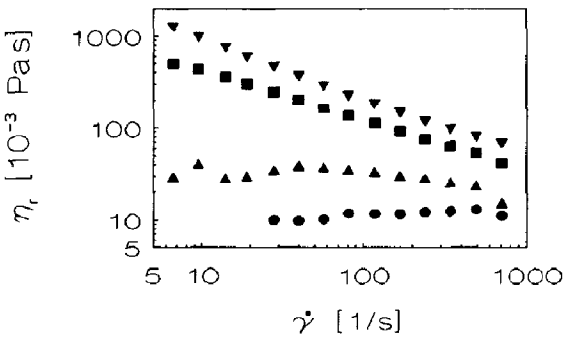

Fig. 3. The apparent viscosity η_r as a function of the shear rate $\dot{\gamma}$ for latexes with the same particle size distribution but with different weight fractions of polymer. The latex was obtained from a batch experiment in Table 1: $f_m = 0.47$, $C_{E0} = 0.132\,kmol/m^3_{water}$, $C_{I0} = 1.2 \times 10^{-2}\,kmol/m^3_{water}$. ●, $f_{pol} = 0.35$; ▲, $f_{pol} = 0.40$; ■, $f_{pol} = 0.45$; ▼, $f_{pol} = 0.47$.

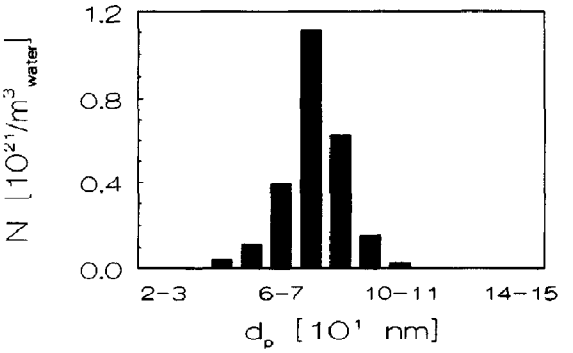

Fig. 4. Particle size distribution of the latexes applied for the rheological measurements presented in Fig. 3.

Table. 1. The particle number and the polymerization rate in interval 2 for the batch emulsion polymerization of styrene at different recipes. $T = 50°C$, $N = 500\,rpm$

f_m	C_{I0} (10^{-2} kmol/m^3_{water})	C_{E0} (10^{-2} kmol/m^3_{water})	R_p [mol/(m^3_{water} s)]	N† (10^{21}/m^3_{water})
0.25	1.3	4.6	0.88	1.6
0.30	1.0	2.8	0.40	0.9
0.30	1.0	1.9	0.30	0.6
0.30	1.3	9.2	1.35	2.4
0.30	1.3	9.2	1.30	2.3
0.35	1.2	19.0	1.12	1.8
0.40	1.2	14.5	1.85	3.2
0.42	2.1	14.8	2.16	4.0
0.40	1.2	23.0	2.28	4.3
0.45	1.2	14.8	1.83	3.4
0.45	2.1	14.8	2.72	4.0
0.45	1.3	9.2	1.83	2.5
0.45	1.2	14.5	2.21	3.2
0.47	1.2	1.2	0.60	0.6
0.47	1.0	2.8	0.78	0.8
0.47	1.2	14.5	2.25	3.6
0.47	1.2	19.0	2.42	4.0
0.47	1.2	23.0	2.76	4.3
0.47	1.2	13.2	2.04	2.5
0.47‡	1.2	13.2	3.4	2.8

† For all experiments the particle number remained constant after the interval of particle nucleation.
‡ Reaction volume is $2.4\,dm^3$.

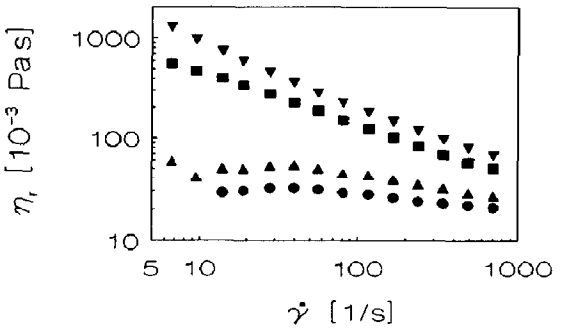

Fig. 5. The apparent viscosity η_r of the reaction mixture as a function of the shear rate $\dot{\gamma}$ at different conversion values for a batch emulsion polymerization of styrene. $f_m = 0.47$, $C_{E0} = 0.132\,\text{kmol/m}^3_{\text{water}}$, $C_{I0} = 1.2 \times 10^{-2}\,\text{kmol/m}^3_{\text{water}}$; ●, $X = 0.05$; ▲, $X = 0.27$; ■, $X = 0.58$; ▼, $X = 0.92$.

stages of the polymerization process, e.g. intervals 2 and 3. The pseudoplastic rheological behaviour observed for the latexes with a volume weight fraction of particles above 0.4 leads to intensive mixing in the impeller zone and an almost stagnant dispersion in the other regions of the tank. In these cases, the rate of heat transfer decreased in the later stages of the process so that a higher cooling capacity was necessary to avoid temperature runaway. However, for polymerizations in the 1.2 dm^3 reactor with monomer weight fractions of 0.47 in the recipe, local hot spots of several degrees Celsius above the desired reactor temperature of 50°C have been observed.

Figure 5 shows the rheological behaviour of the reaction mixture at different conversion values for the batch experiment with a monomer weight fraction of 0.47 in the recipe and the particle size distribution presented in Fig. 4. In Fig. 5, it can be seen that the viscosity of the reaction mixture is still relatively low at conversion values below 0.3. This observation explains the result shown in Fig. 2(a) that the particle number can be predicted with the Smith–Ewart relation, even for recipes with a monomer weight fraction of 0.47: the stage of particle nucleation is finished before heat transfer is limited by insufficient mixing caused by the pseudoplastic behaviour of the reaction mixture.

Figures 6(a) and 6(b), respectively, show the conversion–time history and the particle size distribution at complete conversion, determined with transmission electron microscopy, for a batch experiment where a second generation of particles is formed by the addition of a pulse of emulsifier into the reaction mixture after the stage of particle nucleation. In Fig. 6(a), it can be seen that the polymerization rate increases after addition of the pulse of emulsifier. This increase of the reaction rate results from a second generation of particles formed by micellar nucleation immediately after the addition of emulsifier [see Fig. 6(b)]. In spite of the high monomer weight fraction of 0.47 in the recipe, no heat transfer limitation was observed during the batch experiment with secondary nucleation.

Figure 7 shows the rheological behaviour of the latex product for the batch experiment without secondary nucleation, presented in Fig. 4, and the batch experiment with secondary nucleation for the same monomer weight fraction of 0.47. The particle size distributions of the latex products have already been shown in Figs 4 and 6(b). In Fig. 7, it can be seen that the latex with a bimodal particle size distribution has a significantly lower apparent viscosity at rather low shear rates than the latex with a unimodal particle size distribution and the same polymer content. This explains the result that heat transfer limitation was not observed during the polymerization process with secondary nucleation.

Process in the CSTR

Figures 8(a) and 8(b), respectively, show the course of the particle number and the polymerization rate in the steady state as a function of $(C_{E0} - C_{CMC})\tau^{-2/3}$ [see eq. (3)]. The experimental conditions and some major results are shown in Table 2. Figures 8(a) and 8(b) show that both the particle number and the poly-

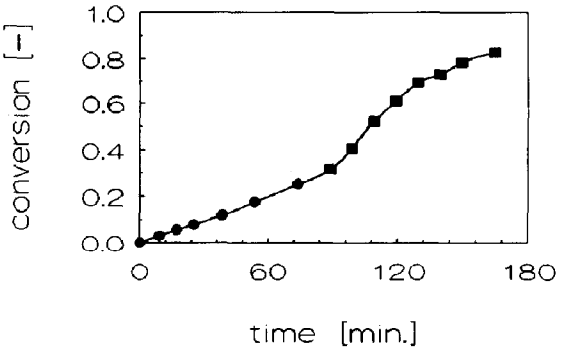

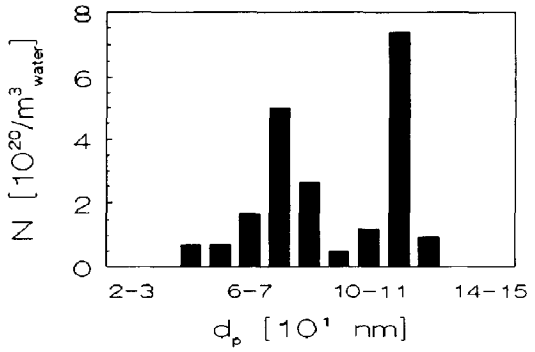

Fig. 6. (a) The conversion as a function of time and (b) the particle size distribution at complete conversion for a batch experiment with secondary nucleation. $T = 50°\text{C}$, $f_m = 0.47$, $C_{E0} = 2.8 \times 10^{-2}\,\text{kmol/m}^3_{\text{water}}$, $C_{I0} = 1.3 \times 10^{-2}\,\text{kmol/m}^3_{\text{water}}$. At $t = 85$ min, the concentration of sodium dodecyl sulphate was increased with $0.13\,\text{kmol/m}^3_{\text{water}}$ by addition of a pulse of emulsifier.

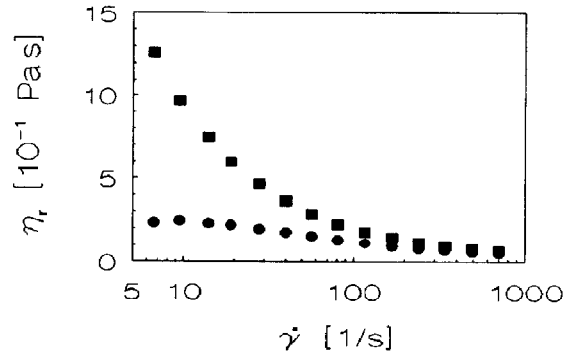

Fig. 7. The apparent viscosity η_r as a function of the shear rate $\dot{\gamma}$ for a batch experiment without secondary nucleation and a batch experiment with secondary nucleation. ■, Batch; ●, Batch with secondary nucleation.

merization rate in the steady state are reasonably well predicted by the model developed by DeGraff and Poehlein [see eq. (3)]. Despite the larger reactor dimensions of the CSTR ($V = 2.4\,dm^3$) compared to the dimensions of the batch reactor ($V = 1.1\,dm^3$), the rate of heat transfer to the reactor wall is sufficient to avoid non-isothermal reactor operation.

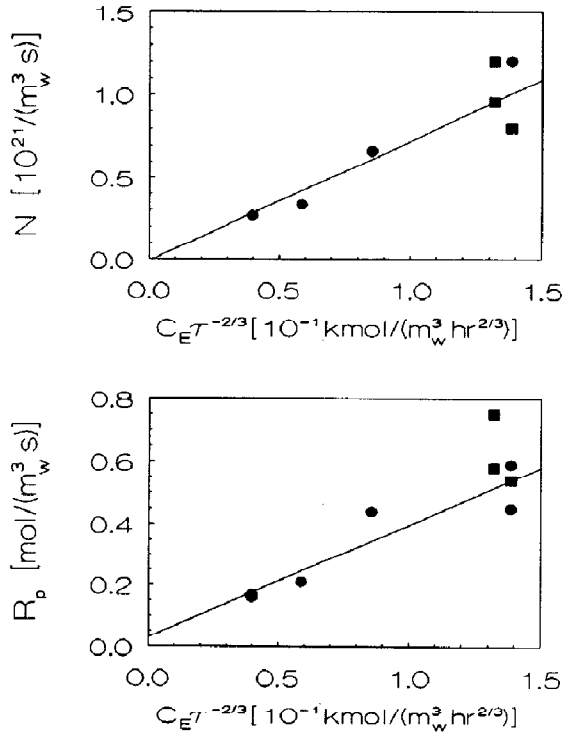

Fig. 8. (a) The particle number N and (b) the polymerization rate in the steady state as a function of the term $(C_{E0} - C_{CMC})\tau^{-2/3}$ for the experiments in a single CSTR listed in Table 2. ●, $f_m < 0.4$; ■, $f_m = 0.47$.

Figure 9 shows the rheological behaviour of the latex product for an experiment in the CSTR (see Table 2), and for the batch experiment in Fig. 5. The particle size distributions of the latex product for the batch experiment and the experiment in the CSTR have been presented in Figs 4 and 10. In Fig. 9, it can be seen that the rather broad particle size distribution in the CSTR, which results from the residence time distribution, leads to a lower viscosity for a given latex concentration as compared to the batch process. This explains the result that the rate of heat transfer was sufficient to provide isothermal reactor operation during the polymerizations in the CSTR.

However, for the experiment listed in Table 2, with a mean residence time in the CSTR of 2.4 h, a significantly higher polymerization rate in the steady state was observed than was predicted with eq. (3), despite the low monomer concentration in the particles (see Table 3).

Table 3 shows the experimentally determined and calculated polymerization rates for the CSTR experiments with $\tau = 2$ h and $\tau = 2.4$ h. The polymerization rates are calculated using eq. (1), the solution of the radical population balance over the particle size distribution [eqs (6)–(10)], and the physical and kinetic parameters are shown in Table 4.

In Table 3 it can be seen that the polymerization rate of the latex with a conversion of 0.75 is significantly higher than the polymerization rate of the latex with the particle size distribution in Fig. 10, and a conversion of 0.48. The observed enhancement of the polymerization rate when the steady-state conversion increases from 0.48 to 0.75 is caused by a gel effect which occurs particularly in the large particles in the reaction mixture. The gel effect finds expression in the apparent termination rate coefficient (k_t), which decreases with conversion (Hawkett *et al.*, 1981). This result shows that reactor operation at steady-state conversions, where a gel effect occurs, may signifi-

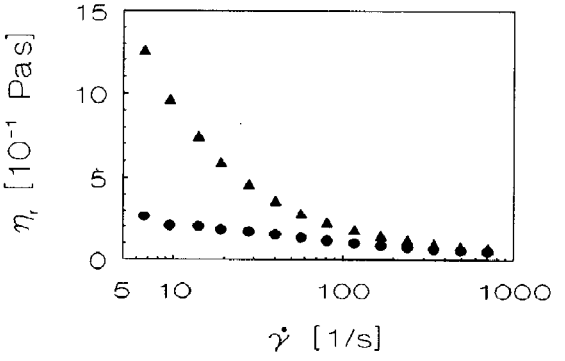

Fig. 9. The apparent viscosity η_r as a function of the shear rate $\dot{\gamma}$ for an experiment in the CSTR listed in Table 2 and the batch experiment in Fig. 5. ▲, Batch experiment; ●, Experiment in the CSTR with $f_m = 0.47$, $C_{E0} = 21.8 \times 10^{-2}$ kmol/m^3_{water}, $C_{I0} = 1.2 \times 10^{-2}$ kmol/m^3_{water} and $\tau = 2$ h.

Table. 2. The particle number and the polymerization rate in the steady state for the emulsion polymerization of styrene in a single CSTR at different recipes. $T = 50°C$, $\tau = 1$ h, $N = 500$ rpm.

f_m	C_{I0} (10^{-2} kmol/m^3_{water})	C_{E0} (10^{-2} kmol/m^3_{water})	X	R_p [mol/(m^3_{water} s)]	N† (10^{21}/m^3_{water})
0.25	1.3	4.6	0.19	0.16	0.3
0.25	1.3	4.6	0.20	0.17	0.3
0.30	1.3	9.2	0.38	0.44	0.7
0.35	1.1	6.5	0.14	0.21	0.3
0.37	1.2	14.5	0.37	0.59	1.2
0.47	1.2	14.5	0.19	0.45	0.8
0.47	1.2	14.5	0.19	0.45	0.8
0.47‡	1.2	21.8	0.48	0.58	0.9
0.47§	1.2	25.3	0.75	0.75	1.2

† During the experiments in the CSTR, no coagulation was observed.
‡ $\tau = 2.0$ h.
§ $\tau = 2.4$ h.

Table. 3. The observed and calculated polymerization rates in the steady state for the experiments in a single CSTR listed in Table 2 with a mean residence time of 2 h and 2.4 h.

τ (h)	X	C_{Mp}(calc) (kmol/m^3)	$\bar{n}$(calc)	R_p(exp) [mol/(m^3_{water} s)]	R_p(calc)† [mol/(m^3_{water} s)]
2.0	0.48	4.76	0.34	0.58	0.63
2.4	0.75	2.41	0.60	0.75	0.73

† Calculated with $f = 0.1$. During all CSTR experiments, a small amount of oxygen present in the feed stream caused some inhibition, reducing the initiator efficiency from 0.5 to 0.1. For the experiments in the batch reactor and the experiments in the PPC, $\bar{n}$ was calculated with $f = 0.5$.

Table. 4. Physical and kinetic parameters for the emulsion polymerization of styrene with sodium persulphate as initiator and sodium lauryl sulphate as emulsifier at 50°C

ρ_m (kg/m^3)	878	Weast (1977)
ρ_p (kg/m^3)	1053	DeGraff and Poehlein (1971)
C_{Mp} (kmol/m^3)	5.2	Harada *et al.* (1972)
k_p [m^3/(kmol s)]	258	Rawlings and Ray (1988)
k_t [m^3/(kmol s)]	$6.8 \times 10^7 \exp(-19\,X^{2.1})$	Hawkett *et al.* (1981)
ρ_i [kmol/(m^3 s)]	$2 f k_i C_I$	Rawlings and Ray (1988)
f	0.5	Rawlings and Ray (1988)
k_i (1/s) (50°C)	1.6×10^{-6}	Rawlings and Ray (1988)
$3\,D_m\,k_{tr}/k_p$ (m^2)	6×10^{-18}	Hawkett *et al.* (1980)

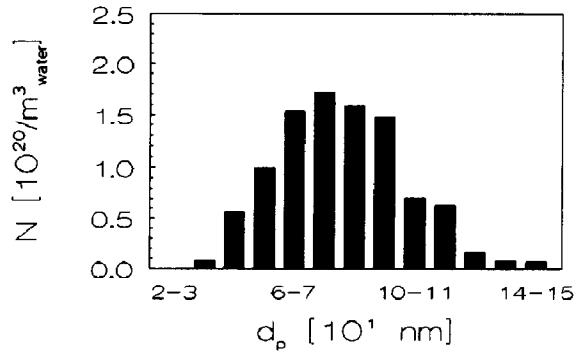

Fig. 10. The particle size distribution in the steady state for the CSTR experiment listed in Table 2 with $\tau = 2$ h. During the sample preparation for TEM analysis, the monomer diffused out of the particles. The particle size distribution presented is based on the amount of polymer present.

cantly enhance the polymerization rate. The model calculations in Table 3 show that the time averaged number of growing chains per particle $\bar{n}$ is considerably enhanced when a gel effect occurs. Both additional CSTR experiments and model calculations with the radical population balance have shown that a small fluctuation in the feed stream may increase the steady-state conversion from 0.5 to 0.8.

Process in the pulsed packed column

Figures 11(a) and 11(b), respectively, show the conversion in the steady state as a function of the mean residence time in the reactor, and the particle size distribution of the latex product for an experiment in the PPC. For the PPC experiment presented in Fig. 11, reactor fouling was negligible and isothermal reactor operation was observed. Figure 11(a) shows that the conversion at the inlet of the column ($z = 0$) differs significantly from zero. This is caused by backmixing.

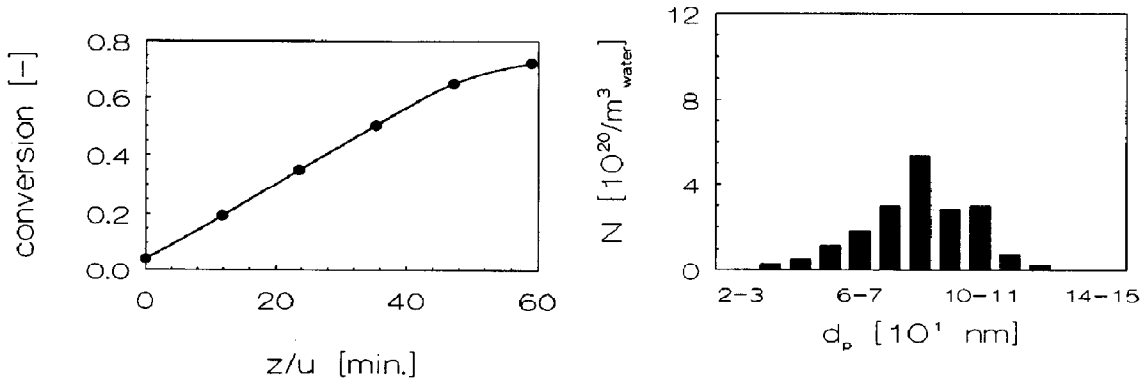

Fig. 11. (a) The conversion as a function of the mean residence time and (b) the particle size distribution of the latex product for an experiment in the PPC. $T = 50°C$, $s = 14$ mm, $f = 3.5$ Hz, $f_m = 0.42$, $C_{E0} = 0.148$ kmol/m$^3_{water}$, $C_{I0} = 2.1 \times 10^{-2}$ kmol/m$^3_{water}$.

Figure 12 shows the rheological behaviour of the latex product for both the PPC experiment in Fig. 11 and the batch experiment in Fig. 13 with the particle size distribution of the latex product presented in Fig. 13. Both experiments were carried out using the same recipe. For the rheological measurements, the volume fraction of the particle phase in the latex product was increased by swelling the particles with styrene until the total particle volume corresponded with that of a latex at complete conversion, with a polystyrene fraction of 0.47.

In Figs 11(b), 12 and 13, it can be seen that even a limited degree of residence time distribution, corresponding with 12 equally sized tanks in series, has a significant effect on both the particle size distribution and the rheological behaviour of the reaction mixture: the apparent viscosity in the PPC is significantly lower than in the batch process. This result shows that the residence time distribution, which can be adjusted in the PPC by changing the pulsation velocity, is a powerful tool to control the particle size distribution and the rheological behaviour of the latex product.

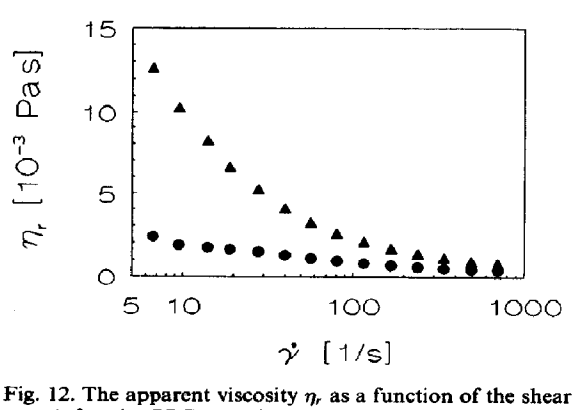

Fig. 12. The apparent viscosity η_r as a function of the shear rate $\dot{\gamma}$ for the PPC experiment in Fig. 11 and the batch experiment in Fig. 13. $T = 50°C$, $f_m = 0.47$, $C_{E0} = 0.148$ kmol/m$^3_{water}$, $C_{I0} = 2.1 \times 10^{-2}$ kmol/m$^3_{water}$. ▲, Batch experiment; ●, Experiment in the PPC.

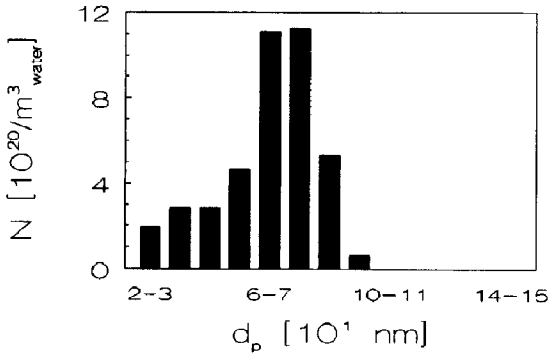

Fig. 13. The particle size distribution of the latex product for a batch experiment listed in Table 1. $f_m = 0.42$, $C_{E0} = 0.148$ kmol/m$^3_{water}$, $C_{I0} = 2.1 \times 10^{-2}$ kmol/m$^3_{water}$.

Figures 14(a) and 14(b), respectively, show the particle number in the latex product and the polymerization rate in the stage where no new particles are formed and the particles grow at the expense of monomer droplets at two different pulsation velocities (sf) for the PPC experiments listed in Table 5. In Fig. 14(a), it can be seen that the particle number in the latex product is considerably lower than that of a batch process with the same recipe. Figure 14(b) shows that the polymerization rate R_p for the batch process in interval 2 is approached at a pulsation velocity $sf = 2.8 \times 10^{-2}$ m/s, even though the particle concentration is significantly lower than in the batch process.

Calculations with the solution of the radical population balance [eqs (6)–(10)] and the physical and kinetic parameters in Table 4, show that the polymerization rate per particle for the largest particles in the column is significantly higher than that for the smallest particles. Obviously, the negative effect of the lower particle concentration on the overall polymerization rate is compensated by a higher average rate of polymerization per particle in the column.

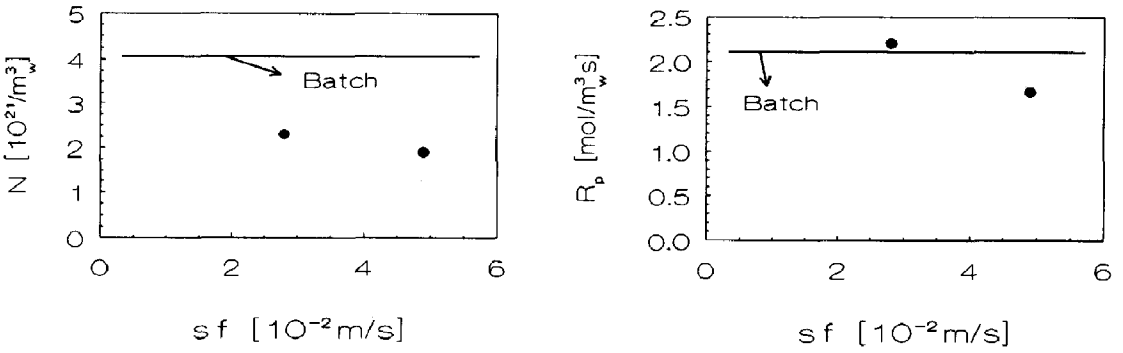

Fig. 14. (a) The particle number N and (b) the polymerization rate R_p as a function of the pulsation velocity sf for the PPC experiments in Table 5

Table. 5. The polymerization rate R_p and the particle number N for experiments in the PPC at two different pulsation velocities sf. $T = 50°C$, $\tau = 1$ h, $C_{E0} = 0.148$ kmol/m$^3_{water}$, $C_{I0} = 0.021$ kmol/m$^3_{water}$, $C_{M0} = 7.5$ kmol/m$^3_{water}$

s (10^{-3} m)	f (1/s)	E† (10^{-4} m^2/s)	R_p‡ [mol/(m$^3_{water}$ s)]	N§ (10^{21}/m$^3_{water}$)
8.0	3.5	1.32	2.2	2.3
14.0	3.5	2.98	1.7	1.9

† Axial mixing coefficient calculated according to Hoedemakers (1990).
‡ Polymerization rates calculated using eq. (4).
§ During the experiments in the PPC, neither reactor fouling nor heat transfer limitation was observed.

CONCLUSIONS

- Experiments with batch emulsion polymerization of styrene show that both the particle number at complete conversion and the polymerization rate in interval 2 are well predicted by the classical Smith–Ewart theory for styrene weight fractions up to 0.4 in the recipe.
- For batch emulsion polymerizations with styrene weight fractions above 0.4 in the recipe, the polymerization rate in interval 2 increases strongly with the monomer content in the recipe and the reactor dimensions. This increase of the reaction rate is caused by the high viscosity and the pseudoplastic rheological behaviour of the latex, leading to imperfect mixing and poor heat transfer to the reactor wall.
- In a batch process, when a second generation of particles is formed by the addition of a pulse of emulsifier into the reaction mixture, heat transfer limitation is avoided. This is caused by the significantly lower viscosity of a latex with a bimodal particle size distribution as compared to a latex with an unimodal particle size distribution and the same polymer content.
- Experiments in a CSTR show that both the particle number and the polymerization rate in the steady state are predicted by the theory of DeGraff and Poehlein for conversions in the steady state below 0.5. For steady-state conversions higher than 0.5, the polymerization rate appeared to be higher than that predicted with the relation of DeGraff and Poehlein. Model calculations with a radical population balance show that these high reaction rates are caused by a gel effect which occurs particularly in the largest particles in the reaction mixture.
- The maximum particle volume at which isothermal reactor operation is possible, depends significantly on the particle size distribution. It was shown that in a PPC, latexes can be prepared that have a much lower viscosity at the same polymer content as compared to those in a batch process. This is caused by a limited degree of backmixing. Therefore, the PPC is a promising reactor for continuous emulsion polymerization provided there is sufficient radial mixing.

Acknowledgements—The authors wish to thank DSM Research BV, Geleen, The Netherlands for the financial support of this study, and students W. G. Boudry, A. J. Bras, E. L. Middelhoek and S. S. G. Pesgens for their contribution to this work.

NOTATION

C_{CMC} critical micelle concentration, kmol/m$^3_{water}$
C_{E0} overall amount of emulsifier in the recipe, kmol/m$^3_{water}$
C_{I0} overall amount of initiator in the recipe, kmol/m$^3_{water}$
C_{M0} overall amount of monomer in the recipe, kmol/m$^3_{water}$

C_{Mp} monomer concentration in the particles, kmol/m^3
C_{rw} radical concentration in the water phase, kmol/m$^3_{water}$
$d_{p,i}$ particle diameter of size class i, m
D_m effective diffusivity of the small radicals, m^2/s
E axial dispersion coefficient, m^2/s
f frequency of pulsation, 1/s
$k_{des,i}$ desorption rate coefficient for particles in size class i, 1/s
k_p propagation rate constant, m^3/(kmol s)
k_t termination rate constant, m^3/(kmol s)
k_{tr} effective chain transfer rate constant, m^3/(kmol s)
k_{tw} termination rate constant for radicals in the water phase, m^3/(kmol s)
$\bar{n}_i$ average number of growing chains of particles in size class i
N_{Av} Avogadro's constant, 1/kmol
N_i number of particles in size class i, 1/m$^3_{water}$
R_p overall polymerization rate, kmol/(m$^3_{water}$ s)
s stroke of pulsation, m
t reaction time, s
u interstitial fluid velocity in the PPC, m/s
$v_{p,i}$ volume of a particle in size class i, m^3
X conversion
z axial coordinate of the PPC

Greek letters

$\dot{\gamma}$ shear rate, 1/s
η_r apparent viscosity, Pa s
ρ_a rate of radical absorption, kmol/(m$^3_{water}$ s)
ρ_i rate of radical formation by initiator decomposition, kmol/(m$^3_{water}$ s)
τ mean residence time in the reactor, s

REFERENCES

Asua, J. M., Sudol, E. D. and El-Aasser, M. S., 1991, Radical desorption in emulsion polymerization. *J. Polym. Sci. Part A* **27**, 3903–3913.

DeGraff, A. W. and Poehlein, G. W., 1971, Emulsion polymerization of styrene in a single continuous stirred-tank reactor. *J. Polym. Sci. Part 2-A* **9**, 1955–1976.

Friis, N. and Nyhagen, L., 1973, A kinetic study of the emulsion polymerization of vinyl acetate. *J. Appl. Polym. Sci.* **17**, 2311–2327.

Harada, M., Nomura, M., Kojima, H., Eguchi, W. and Nagata, S., 1972, Rate of emulsion polymerization of styrene. *J. Appl. Polym. Sci.* **16**, 811–833.

Hawkett, B. S., Napper, D. H. and Gilbert, R. H., 1980, Seeded emulsion polymerization of styrene. *J. Chem. Soc. Faraday Trans 1* **76**, 1323–1343.

Hawkett, B. S., Napper, D. H. and Gilbert, R. G., 1981, Analysis of interval III data for emulsion polymerization. *J. Chem. Soc. Faraday Trans 1* **77**, 2395–2404.

Hoedemakers, G. F. M., 1990, Continuous emulsion polymerization in a pulsed packed column. Ph.D. thesis, Eindhoven University of Technology.

Hoedemakers, G. F. M. and Thoenes, D., 1990, Continuous emulsion polymerization in a pulsed packed column, in *Integration of Fundamental Polymer Science and Technology* (Edited by P. J. Lemstra and L. A. Kleintjes), pp. 182–193. Elsevier, London.

Mayer, M. J. J., 1995, The dynamics of batch and continuous emulsion polymerization. Ph.D. thesis, Eindhoven University of Technology.

Meuldijk, J., van Strien, C. J. G., van Doormalen, F. A. H. C. and Thoenes, D., 1992, A novel reactor for continuous emulsion polymerization. *Chem. Engng Sci.* **47**, 2603–2608.

Mooney, M. J., 1951, The viscosity of a concentrated suspension of spherical particles. *J. Colloid. Sci.* **6**, 162–170.

Nomura, M. and Harada, M., 1981, Rate coefficient for radical desorption in emulsion polymerization. *J. Appl. Polym. Sci.* **26**, 17–26

Nomura, M., Kojima, H., Harada, M., Eguchi, W. and Nagata, S., 1971, Continuous flow operation in emulsion polymerization of styrene. *J. Appl. Polym. Sci.* **15**, 675–691.

O'Toole, J. T., 1965, Kinetics of emulsion polymerization. *J. Appl. Polym. Sci.* **9**, 1291–1297.

Rawlings, J. B. and Ray, W. H., 1988, The modeling of batch and continuous emulsion polymerization reactors. Part II: Comparison with experimental data from continuous stirred tank reactors. *Polym. Engng Sci.* **28**, 257–274.

Sadler, L. Y. and Sim, K. G., 1991, Minimize solid–liquid mixture viscosity by optimizing particle size distribution. *Chem. Engng Prog.*, 68–71.

Smith, W. V. and Ewart, R. H., 1948, Kinetics of emulsion polymerization. *J. Chem. Phys.* **16**, 592–599.

Stockmayer, W. H., 1957, Note on the kinetics of emulsion polymerization. *J. Polym. Sci.* **24**, 314–317.

Ugelstad, J., Mörk, P. C. and Aassen, J. O., 1967, Kinetics of emulsion polymerization. *J. Polym. Sci., A1* **5**, 2281–2288.

Weast, R. C., 1977, *Handbook of Chemistry and Physics*. CRC Press, New York.